

Figure S1 The detailed view of the applied periodic (left) and cluster models (right) on example of *cis*- $S_4Na_7Cl(Si_6Al_6O_{24})$ model (48 atoms/unit cell). The cluster cut from the periodic structure consists of the whole truncated cubooctahedral SOD cage with S_4 species inside. The dangling O atoms in cluster model are saturated with H atoms, put along the line of broken O—Si/Al bond. The formula of cluster is $(S_4Na_7Si_{12}Al_{12}O_{60}H_{24})^{-5}$. Atom coloration (as used in whole paper): S — yellow, Na — purple, O — red, Si/Al — dark/light blue, H — white (cluster model only), Cl — green.

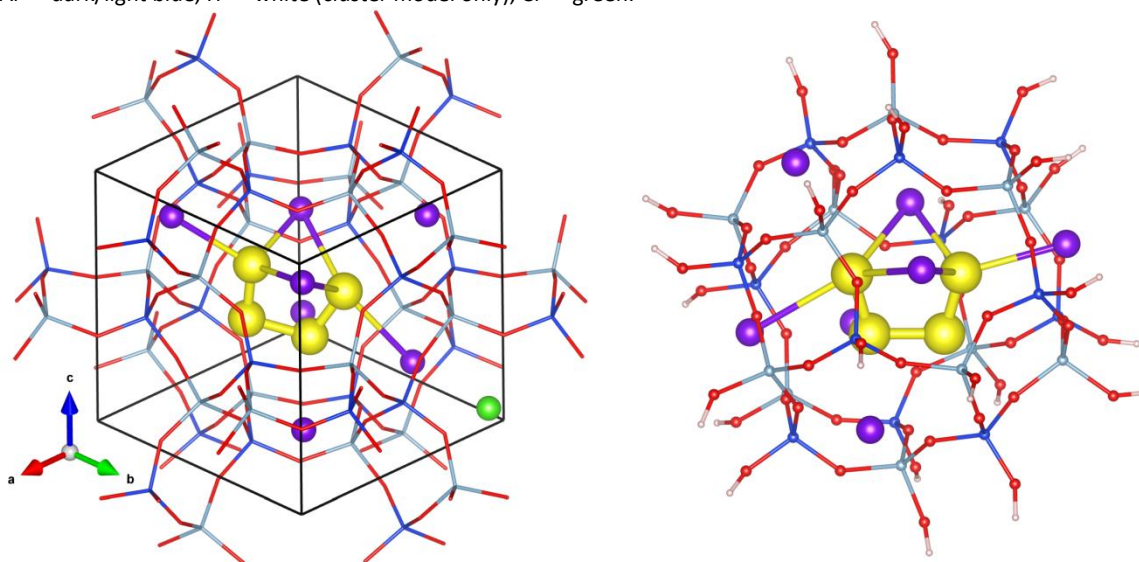


Figure S2 Broken spin symmetry singlet solutions for *cis*- C_{2v} (top) and *trans*- C_{2h} (bottom) isomers of S_4 : plots of the highest occupied orbitals for both spin components (left and middle) and spin density (right). Broken spin solutions are of 6 and 16 kJ/mol lower energy than the restricted solutions for *cis* and *trans* isomer, respectively. The values of S^2 are 0.46 and 0.66 for *cis* and *trans* isomer, respectively.

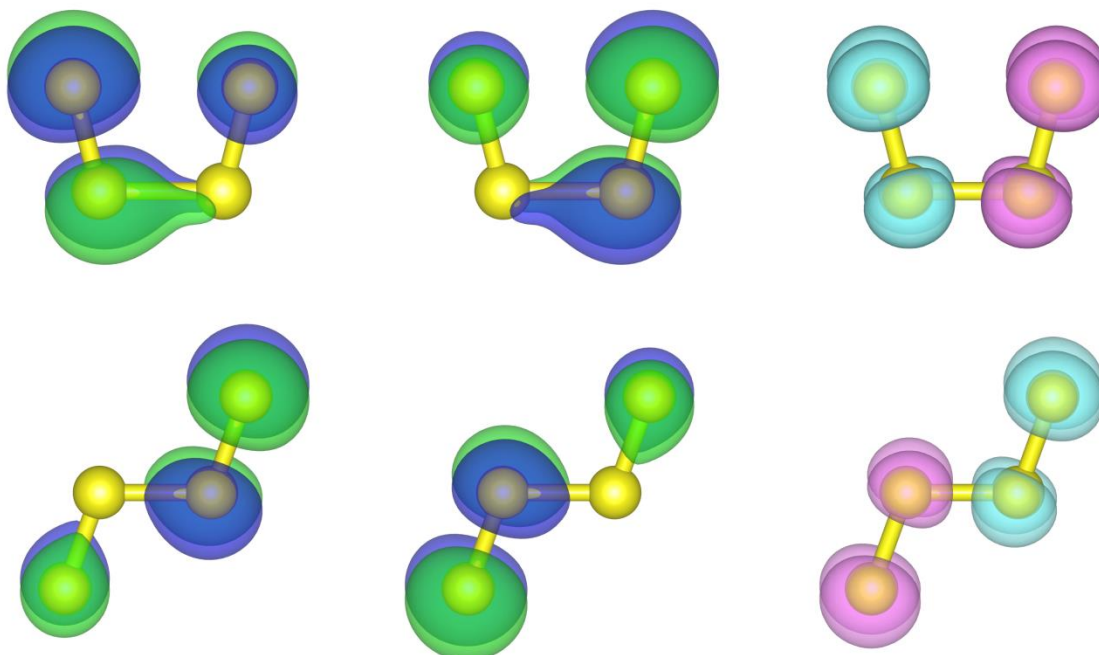


Table S1 DFT/B3LYP results for the isomers of isolated S_4 and $S_4^{\bullet\bullet}$ species: bond lengths (R, in Å), bond angles (Θ , in $^\circ$) and relative energetic stabilities (ΔE , in kJ/mol). See Figure 1 in main text for atom labeling.

	S_4					
	<i>cis</i> - C_{2v}	<i>trans</i> - C_{2h}	D_{2h}	C_s	D_{2d}	D_{3h}
	def2-TZVP/def2-QZVPP					
$R_{S1-S2/S1'}$	1.915/1.917	1.931/1.933	1.897/1.902	1.909/1.911	2.131/2.138	1.914/-
$R_{S2-S2'}$	2.121/2.129	2.079/2.080	2.558/2.543	2.177/2.180		
$\Theta_{122'}$	107.55/107.02	111.31/111.41	90.00	116.35/116.45	85.00/85.08	120.00/-
$R_{S3-S3'}$	-	-	-	2.111/2.114	-	-
ΔE	0	28/27	15/16	57/57	80/80	88/89

	$S_4^{\bullet\bullet}$				
	<i>cis</i> - C_{2v}	<i>trans</i> - C_{2h}	D_{2h}	C_{3v}	C_s
	ma-def2-TZVP/ma-def2-QZVPP				
R_{S1-S2}	1.978/1.980	2.002/2.001	1.953/1.956	2.001/2.004	1.996/2.000
$R_{S2-S2'}$	2.213/2.216	2.138/2.135	2.692/2.698	-	2.087/2.088
$\Theta_{122'}$	109.55/109.38	108.72/108.75	90.00/90.00	115.87/115.87	113.43/113.11
$R_{S3-S3'}$	-	-	-	-	2.835/2.838
ΔE	3/3	0/0	21/23	71/70	92/92

Table S2 The multireference diagnostics obtained for $S_4/S_4^{\bullet\bullet}$ species: CASSCF natural orbital occupation numbers (NOON), CCSD(T) maximum norm of double amplitudes ($|t_2|_{\max}$) and T_1 diagnostics, along with the stability test of unrestricted Kohn-Sham solutions for singlet S_4 . NOONs for S_4 HOMO/LUMO and $S_4^{\bullet\bullet}$ SOMO are underlined, the values deviating by more than 0.1 from the single configuration integer occupation depicted in bold. The character of excited configuration corresponding to $|t_2|_{\max}$ given in parenthesis.

Isomer	NOON	$ t_2 _{\max}$	T_1	UKS stability PBE/B3LYP
S_4				
<i>cis</i> - C_{2v}	1.954, 1.756 , 0.298 , 0.085	0.178 (HOMO \boxtimes LUMO)	0.023	Y/N
<i>trans</i> - C_{2h}	1.957, 1.692 , 0.354 , 0.070	0.188 (HOMO \boxtimes LUMO)	0.024	N/N
C_s	1.944, <u>1.943</u> , <u>0.089</u> , 0.066	0.047 (HOMO-5 \boxtimes LUMO)	0.024	Y/Y
D_{2d}	1.958, 1.958, <u>1.957</u> , <u>0.046</u> , <u>0.046</u>	0.062 (HOMO-3/-4 \boxtimes LUMO+2)	0.015	Y/Y
D_{3h}	1.965, 1.965, <u>1.944</u> , <u>1.944</u> , 0.126 , 0.043	0.162 (HOMO-1/-2 \boxtimes LUMO+2)	0.019	Y/Y
$S_4^{\bullet\bullet}$				
<i>cis</i> - C_{2v}	1.961, 1.940, <u>1.059</u> , 0.095, 0.039	0.052 (SOMO-1 \boxtimes SOMO, SOMO-2 \boxtimes SOMO+12)	0.023	-
<i>trans</i> - C_{2h}	1.967, 1.947, <u>1.050</u> , 0.078, 0.036	0.043 (SOMO-1 \boxtimes SOMO, SOMO-2 \boxtimes SOMO+12)	0.024	-
D_{2h}	1.933, 1.897 , <u>1.088</u> , 0.180 , 0.027	0.082 (SOMO-1 \boxtimes SOMO, SOMO-2 \boxtimes SOMO+5)	0.014	-
C_{3v}	1.963, 1.963, <u>1.029</u> , 0.059, 0.038, 0.038	0.022 (SOMO-1 \boxtimes SOMO+11, SOMO-7 \boxtimes SOMO)	0.023	-
C_s	1.959, 1.957, <u>1.029</u> , 0.059, 0.056	0.030 (SOMO-1 \boxtimes SOMO, SOMO-1 \boxtimes SOMO+15)	0.025	-

Table S3 The DFT/PBE calculated unit cell parameters for S_4/S_4^{\bullet} hosting sodalite lattices. For comparison also experimental and computed data for pristine sodalite are given.

	S_4Na_8Ssod		$S_4Na_7Cl sod$		
	<i>cis</i> - C_{2v}	<i>gauche</i> - C_2^1	C_s	D_{2d}	D_{3h}
V_{cell} (\AA^3)	737.47	757.41	733.51	753.05	749.78
a, b, c (\AA)	9.025, 9.030, 9.050	9.076, 9.091, 9.181	8.999, 8.998, 9.060	9.139, 9.111, 9.044	9.047, 9.039, 9.169
α, β, γ ($^\circ$)	90.00, 90.00, 90.51	89.53, 88.97, 89.89	90.66, 90.71, 90.07	90.00, 90.00, 90.00	89.46, 90.10, 89.52
	$S_4Na_7Cl sod$		$S_4^{\bullet}Na_8Cl-sod$		
	<i>cis</i> - C_{2v}	<i>trans</i> - C_{2h}	C_s	D_{2d}	D_{3h}
V_{cell} (\AA^3)	739.96	764.38	738.69	757.11	762.57
a, b, c (\AA)	9.061, 9.059, 9.016	9.061, 9.089, 9.074	9.006, 9.044, 9.069	9.148, 9.115, 9.080	9.047, 9.039, 9.169
α, β, γ ($^\circ$)	90.34, 89.66, 90.81	90.86, 89.59, 90.41	89.31, 90.13, 90.11	90.43, 90.30, 89.96	89.46, 90.10, 89.52
	$S_4^{\bullet}Na_8Cl-sod$		$S_4^{\bullet}Na_7sod$		
	<i>cis</i> - $C_{2v}-1$	<i>cis</i> - $C_{2v}-2$	C_s	C_{3v}	C_{3v}
V_{cell} (\AA^3)	760.06	753.91	744.67	742.58	749.22
a, b, c (\AA)	9.100, 9.172, 9.108	9.059, 9.090, 9.156	9.065, 9.050, 9.080	9.032, 9.028, 9.107	9.082, 9.083, 9.083
α, β, γ ($^\circ$)	89.44, 89.12, 89.36	90.00, 90.00, 90.81	89.95, 88.86, 89.94	89.42, 89.43, 89.98	89.49, 89.49, 90.51
	$S_4^{\bullet}Na_7sod$		Sodalite (<i>P-43n</i>)		
	<i>cis</i> - $C_{2v}-1$	<i>cis</i> - $C_{2v}-2$	C_{3v}	-	-
V_{cell} (\AA^3)	775.39	770.85	778.39	-	-
a, b, c (\AA)	9.226, 9.151, 9.186	9.204, 9.163, 9.141	9.237, 9.243, 9.118	-	-
α, β, γ ($^\circ$)	90.28, 88.67, 89.95	89.61, 89.18, 89.68	89.60, 89.74, 90.91	-	-
	Exp. ^b		DFT		
V_{cell} (\AA^3)	699.05		707.63		
a, b, c (\AA)	8.875		8.911		
α, β, γ ($^\circ$)	90.0		90.0		

^aConverged from initial C_{2h} geometry. ^bI. Hassan and H. D. Grundy, *Acta Crystallogr. B*, 1984, **40**, 6–13.

Table S4 The supplement to Table 4 in main text: number of lattice O ions coordinating S atoms (CN) and the range of S-O distance (R, in \AA) within 3.40 \AA radius. O ions bound to more than one S atoms underlined.

	S_4 models		S_4^{\bullet} models	
	<i>cis</i> S_4Na_8Ssod	<i>cis</i> $S_4Na_7Cl sod$	<i>cis</i> $S_4^{\bullet}Na_8Cl sod$	<i>cis</i> $S_4^{\bullet}Na_7sod$
CN $_{S1-O}/R_{S1-O}$	3/3.196–3.290	1/3.349	2/3.097, 3.343	1/3.269
CN $_{S1'-O}/R_{S1'-O}$	3/3.196–3.290	3/3.169, 3.196, <u>3.299</u>	3/3.250, 3.279, 3.343	2/3.284, 3.390
CN $_{S2-O}/R_{S2-O}$	3/3.164–3.377	2/3.048, <u>3.182</u>	3/3.298, 3.328, 3.387	3/3.317, 3.332, 3.387
CN $_{S2'-O}/R_{S2'-O}$	3/3.164–3.377	4/2.955, 2.971, <u>3.108</u> , 3.387	2/3.198, 3.346	3/3.304, 3.339, 3.368

Table S5 The DFT/PBE data obtained for S_4 species embedded in periodic models: bond lengths (R, in Å), bond angles and torsions (Θ and ϕ , in °), total numbers of Na ions coordinating S_4 molecule ($CN_{(S_4)-Na}$), numbers of Na and O ions coordinating S atoms ($CN_{Sx-Na/O}$) and Bader electronic charges (Q). The coordination distances set to 3.40 Å. $R_{intermol}$ denotes the nearest distance between S_4 species occupying adjacent SOD cages. For atom and bond angles numbering see Figure 1 in main text.

	$trans-C_{2h}^a$	C_s	D_{2d}	D_{3h}
	S_4Na_8Ssod			
R_{S1-S2}	1.940, 1.980	1.937	2.118, 2.154	1.916, 1.936, 1.945
$R_{S2-S2'/S2-S3, S2-S3'}$	2.076	2.144, 2.148	–	–
$\Theta_{122', 1'2'2/123, 123'}$	104.47, 103.99	111.16, 111.20	85.20	120.50, 117.53, 121.90
$R_{S3-S3'}$	–	2.101	–	–
$\Theta_{323'}$	–	58.62	–	–
$\phi_{122'1'/11'1''3}$	134.75	–	32.57	1.706
total $CN_{(S_4)-Na}$	5	3	4	4
$S_x CN_{Sx-Na}/R_{Sx-Na}$	S1 1/2.987 S1' 2/2.979, 2.855 S2 0/– S2' 2/2.986, 2.973	S1 3/2.956, ^b 3.031, 3.299 S2 0/– S3 1/3.248 S3' 3.116	1/2.904	S1 0/– S1' 2/2.867, 3.246 S1'' 1/2.814 S2 1/3.278
$S_x: CN_{Sx-O}/R_{Sx-O}^3$	S1 5/2.623–3.364 S1' 5/2.626–3.324 S2, S2' 0/–	S1 3/3.069–3.267 S2 0/– S3 2/3.018, 3.174 S3' 3/3.038–3.347	1/3.146	S1 2/2.728, 3.056 S1' 2/2.729, 3.166 S1'' 3/2.882–3.399 S2 0/–
$R_{intermol}$	6.338 (S1–S1')	6.839 (S1–S3')	7.075	6.122 (S1–S1')
$S_x Q_{Sx}$	S1 -0.08, S1' -0.25 S2 0.03, S2' -0.16	S1 -0.25, S2 0.24 S3 -0.03, S3' -0.03	S1-S1''' -0.03	S1 -0.01, S1' -0.10, S1'' -0.01, S3 -0.03
	S_4Na_7ClSod			
R_{S1-S2}	1.892, 2.003	1.957	2.123, 2.125, 2.148, 2.154	1.925, 1.933, 1.933
$R_{S2-S2'/S2-S3, S2-S3'}$	2.107	2.133, 2.136	–	–
$\Theta_{122', 1'2'2/123, 123'}$	109.26, 103.04	111.45, 115.62	83.51, 86.72, 82.23, 83.64	119.35, 118.82, 121.81
$R_{S3-S3'}$	–	2.106	–	–
$\Theta_{323'}$	–	59.10	–	–
$\phi_{122'1'/11'1''3}$	174.75	–	33.83	178.36
total $CN_{(S_4)-Na}$	4	4	4	6
$S_x CN_{Sx-Na}/R_{Sx-Na}$	S1 0/– S1' 2/2.794, 3.054 S2 1/3.364 S2' 2/2.836, 2.856	S1 2/2.792, 2.971 S2 1/3.020 S3 2/3.247, 3.261 S3' 0/–	S1 1/3.239 S1' 2/2.808, 3.179 S1'' 1/3.346 S1''' 2/2.812, 3.150	S1 1/3.247 S1' 2/2.824, 3.218 S1'' 1/2.873 S3 1/3.378
$S_x CN_{Sx-O}/R_{Sx-O}^c$	S1 6/2.414–3.350 S1' 3/2.869–3.312 S2 1/3.212 S2' 0/–	S1 1/3.159 S2 0/– S3 3/2.834–3.315 S3' 4/2.602–3.358	S1 0/– S1' 2/3.162, 3.173 S1'' 3/2.845–3.382 S1''' 2/3.181, 3.223	S1 2/2.843, 3.114 S1' 3/2.724–3.382 S1'' 2/2.836, 3.188 S3 0/–
$R_{intermol}$	6.951 (S1–S1')	6.681 (S1–S3)	7.001 (S1–S1''')	6.576 (S1–S1')
$S_x Q_{Sx}$	S1 0.24, S1' -0.40, S2 -0.06, S2' -0.16	S1 -0.31, S2 0.12, S3 -0.05, S3' 0.11	S1 -0.03, S1' -0.07, S1'' 0.07, S1''' -0.08	S1 -0.04, S1' -0.06, S1'' -0.03, S2 -0.01

^aIn the case of model converged to *gauche*- C_2 like structure (actual symmetry C_1). ^bUnderlining depicts the Na ions bound to more than one S atoms. ^cFor more than two O atoms in the vicinity of S atoms only the range of S–O distances is given.

Table S6 The DFT/PBE data obtained for $S_4^{\bullet-}$ species embedded in periodic models: bond lengths (R, in Å), bond angles and torsions (Θ and ϕ , in $^\circ$), total numbers of Na ions coordinating S_4 molecule ($CN_{(S_4)-Na}$), numbers of Na and O ions coordinating S atoms ($CN_{Sx-Na/O}$), Bader electronic (Q) and spin ($N^{\alpha-\beta}$) charges. The coordination distances set to 3.40 Å. $R_{intermol}$ denotes the nearest distance between S_4 species occupying adjacent SOD cages. For atom and bond angles numbering see Figure 1 in main text.

	$(S_4^{\bullet-})Na_8ClSod$			
	<i>cis</i> - C_{2v} -2	<i>gauche</i> - C_2	C_s	C_{3v}
R_{S1-S2}	1.961, 1.961	2.004, 2.008	1.975	1.973
$R_{S2-S2'/S2-S3, S2-S3'}$	2.232	2.130	2.065, 2.066	–
$\Theta_{122', 1'2'/123, 123'}$	101.72, 101.72	97.58, 96.56	108.99, 109.29	115.00
$R_{S3-S3'}$	–	–	2.766	–
$\Theta_{323'}$	–	–	84.06	–
$\phi_{122'1'/11'1''3}$	2.77	70.79	–	25.00
total $CN_{(S_4^{\bullet-})-Na}$	6	6	7	7
$S_x CN_{Sx-Na}/R_{Sx-Na}$	S1 3/ <u>2.902</u> , ^a 2.939, <u>3.031</u> S2 1/3.013	S1 4/ <u>2.989</u> , 3.104, <u>3.116</u> , 3.299 S1' 3/ <u>2.941</u> , 3.020, <u>3.132</u> S2 2/ <u>2.741</u> , <u>3.021</u> S2' 2/2.742, 2.997	S1 4/ <u>2.925</u> , <u>2.926</u> , 3.268, <u>3.386</u> S2 2/ <u>3.073</u> , <u>3.076</u> S3 4/ <u>2.896</u> , <u>3.028</u> , <u>3.255</u> , 3.314 S3' 4/ <u>2.893</u> , <u>3.043</u> , <u>3.255</u> , 3.307	S1 3/ <u>2.873</u> , <u>2.900</u> , 3.187 S2 1/2.901
$S_x: CN_{Sx-O}/R_{Sx-O}$ ^b	S1 3/3.185–3.363 S2 1/3.251	S1 3/3.095–3.158 S1' 3/2.998–3.173 S2 1/3.397 S2' 2/3.284, 3.395	S1 2/3.074, 3.086 S2 0/– S3 3/3.111, 3.265, 3.314 S3 3/3.115, 3.231, 3.277	S1 3/3.090, 3.138, 3.375 S2 0/–
$R_{intermol}$	7.058 (S1–S1')	6.871 (S1–S1')	6.817 (S1–S3')	7.100 (S1–S1)
$S_x Q_{Sx}/N^{\alpha-\beta}_{Sx}$	S1 -0.36/0.21 S2 -0.06/0.27	S1, S1' -0.11/0.35 S2, S2' -0.33/0.15	S1 -0.40/0.00 S2 0.11/0.00 S3, S3' -0.30/0.48	S1 -0.31/0.24 S2 0.05/0.22

	$(S_4^{\bullet-})Na_7sod$	
	<i>cis</i> - C_{2v} -2	C_{3v}
R_{S1-S2}	1.940, 1.980	1.964, 1.994, 1.995
$R_{S2-S2'/S2-S3, S2-S3'}$	2.254	–
$\Theta_{122', 1'2'/123, 123'}$	100.01, 102.03	115.72, 109.37, 116.09
$\phi_{122'1'/11'1''3}$	3.89	26.00
total $CN_{(S_4^{\bullet-})-Na}$	6	6
$S_x CN_{Sx-Na}/R_{Sx-Na}$	S1 2/ <u>2.826</u> , 2.829 S1' 3/2.832, <u>2.945</u> , <u>3.076</u> S2 0/– S2' 3/2.762, 3.168, <u>3.213</u>	S1 1/ <u>3.214</u> S1' 3/2.903, <u>2.906</u> , <u>2.929</u> S1'' 3/2.844, 2.917, <u>3.048</u> S3 1/3.245
$S_x CN_{Sx-O}/\{R_{Sx-O}\}^Y$	S1 5/3.055–3.399, S1' 2/3.293, 3.338 S2 3/3.233–288, S2' 1/3.342	S1 3/3.080–3.350, S1' 5/3.186–3.385 S1'' 2/3.069, 3.250, S3 0/–
$R_{intermol}$	6.520 (S1–S2')	6.462 (S1–S1'')
$S_x Q_{Sx}/N^{\alpha-\beta}_{Sx}$	S1 -0.31/0.30 S1' -0.40/0.16 S2 0.04/0.33 S2' -0.20/0.18	S1 -0.17/0.33, S1, S1'' -0.40/0.19 S2 0.06/0.22

^aUnderlining depicts the Na^+ ions bound to more than one S atoms. ^bFor more than two O atoms in the vicinity of S atoms only the range of S - O distances is given.

Figure S3 DFT frontier orbitals for gas phase S_4 isomers.

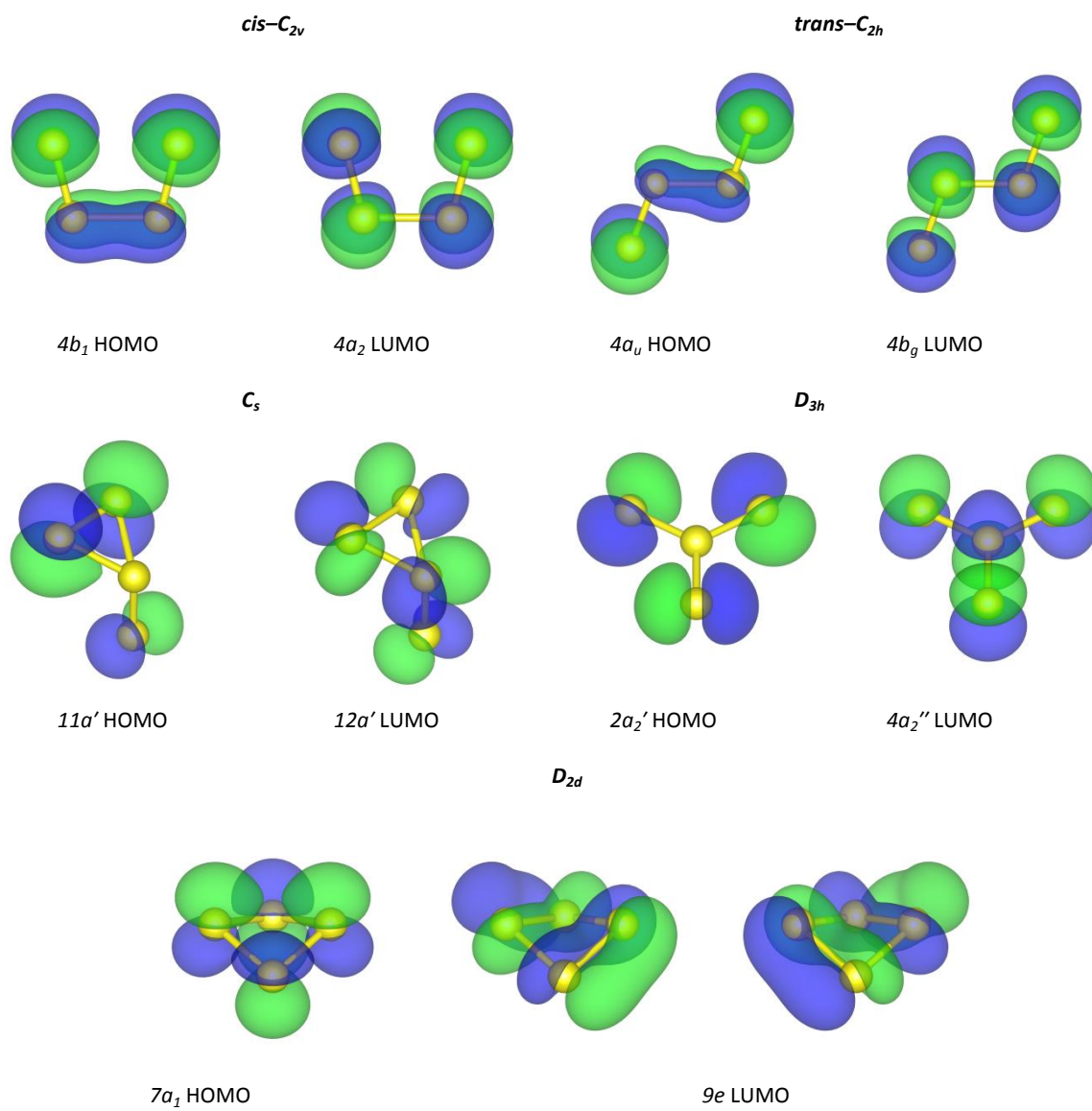


Figure S4 The most relevant for optical transitions (see Table 7 in main text) MOs of gas phase S_4^{\bullet} radical.

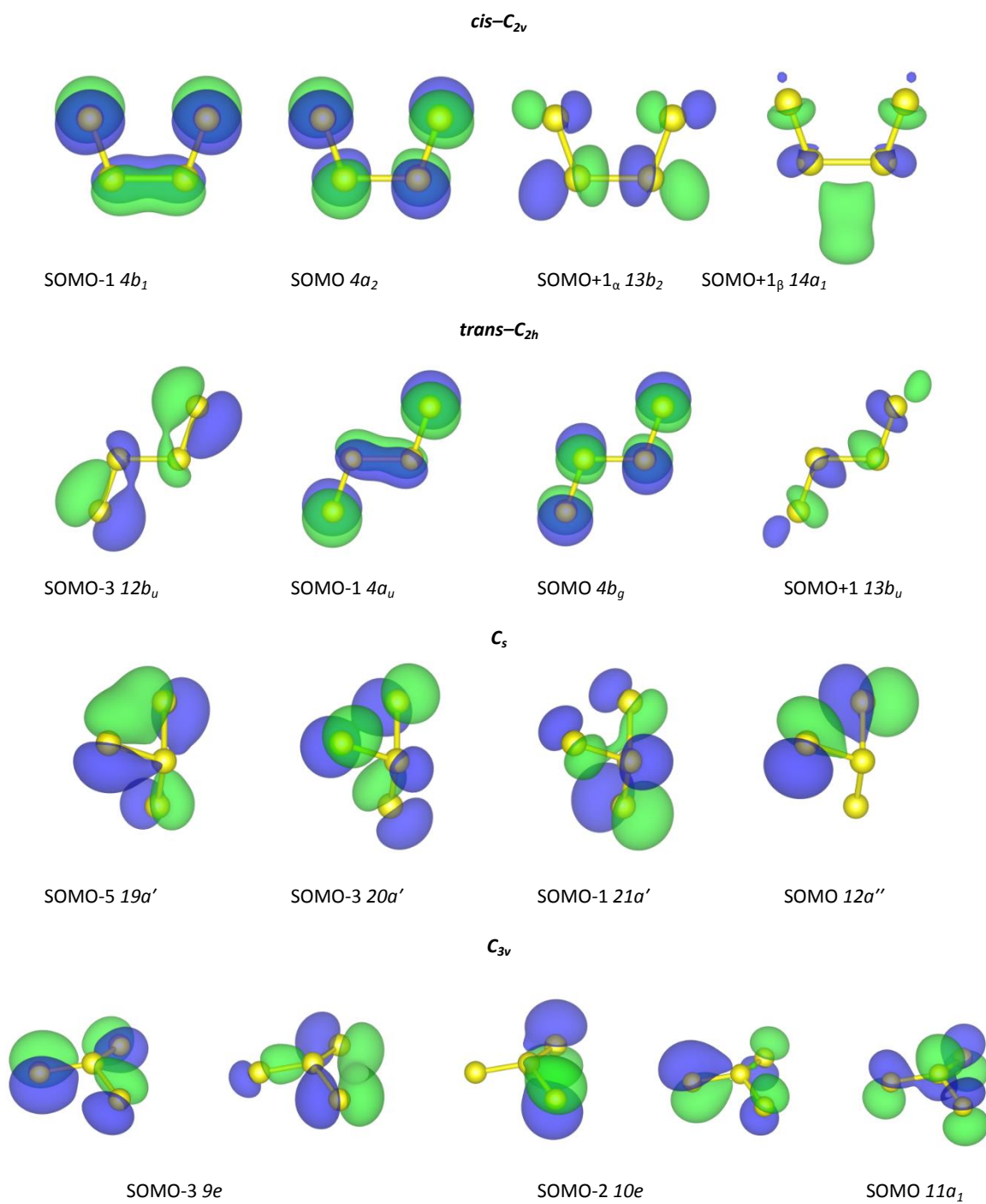


Table S7 TDDFT/LC-BLYP electronic transitions within the range of 350-800 nm for S_4 chromophores embedded in SOD cages: wavelengths λ and oscillator strengths f_{osc} (in parenthesis), along with the dominant orbital contribution are given. The S_4 isomers and the relevant orbitals are labeled according to the ideal symmetry of the corresponding gas phase S_4 species (compare with Table 6 in manuscript), even if the actual symmetry of embedded is lower.

S_4 isomer	λ (nm), f_{osc}	TDDFT excitation character
<i>cis</i> - C_{2v}	507 (0.120)	(S_4) Na_8Ssod $4b_1$ /HOMO/ \rightarrow $4a_2$ /LUMO/ (76%) $13a_1$ /HOMO-2/ \rightarrow $13b_2$ /LUMO+1/ (22%)
	371 (0.044)	$O\ 2p \rightarrow 4b_g$ /LUMO/ ^d
<i>gauche</i> - C_2 (C_1) ^{a,b}	704 (0.179)	$17a$ /HOMO/ \rightarrow $4b$ /LUMO/ (66%) ^c $16a$ /HOMO-1/ \rightarrow $16b$ /LUMO+1/ (10%) ^c
	371 (0.044)	$O\ 2p \rightarrow 4b_g$ /LUMO/ ^d
C_s	475 (0.002)	$11a''$ /HOMO/ \rightarrow $12a''$ /LUMO/ S_4 (74%) ^e $10a''$ /HOMO-2/ \rightarrow $12a''$ /LUMO/ S_4 (17%)
	361 (0.003)	$21a'$ /HOMO-1/ \rightarrow $12a''$ /LUMO/ S_4 (85%)
D_{2d} (D_2)	591 (0.002)	$7a_1$ /HOMO/ \rightarrow $9e(1)$ /LUMO/ (92%) ^f
	517 (0.002)	$7a_1$ /HOMO/ \rightarrow $9e(2)$ /LUMO+1/4 (92%) ^f
D_{3h} (C_1)	356 (0.158)	$2e'$ (+ $O\ 2p$) /HOMO-1/ \rightarrow $4a_2''$ /LUMO/ (>60%) ^g
	352 (0.166)	
<i>cis</i> - C_{2v}	478 (0.147)	(S_4) $Na_7Clisod$ $4b_1$ /HOMO/ \rightarrow $4a_2$ /LUMO/ (83%)
	393 (0.006)	π^*_{S1-S2} /HOMO/ \rightarrow π^*_{S1-S2} /LUMO/ S_4 (78%) ^h $12b_u$ (+ $O\ 2p$) /HOMO-2/ \rightarrow π^*_{S1-S2} /LUMO/ S_4 (36%) $13a_g$ /HOMO-1/ \rightarrow π^*_{S1-S2} /LUMO/ S_4 (35%)
C_s	502 (0.003)	$11a''$ /HOMO/ \rightarrow $12a''$ /LUMO/ S_4 (74%)
D_{2d} (C_1)	509 (0.002)	$7a_1$ /HOMO/ \rightarrow $9a_2$ /LUMO/ S_4 (44%) ^f $7a_1$ /HOMO/ \rightarrow $9e(1)$ /LUMO+1/ S_4 (37%) ^f
	482 (0.003)	$7a_1$ /HOMO/ \rightarrow $9e(2)$ /LUMO+2/ S_4 (64%) $7a_1$ /HOMO/ \rightarrow $9e(1)$ /LUMO+1/ S_4 (16%)
D_{3h}	359 (0.159)	$2e'$ /HOMO/ \rightarrow $4a_2''$ /LUMO/ S_4 (31%) $O\ 2p \rightarrow 4a_2''$ /LUMO/ S_4 (>36%)

^aConverged from initial C_{2h} geometry. ^bThe actual symmetry of embedded molecule in parenthesis. ^cWithin twisted *gauche*- C_2 geometry orbitals $16a$, $17a$ (HOMO) and $16b$ (LUMO) correspond to $13a_g$, $4a_u$ and $4b_g$ orbitals, respectively, of the planar C_{2h} isomer. ^dCharge transfer between lattice $O\ 2p$ states and LUMO localized at S_4 , see Figure S5. ^eLUMO $_{S_4}$ denotes LUMO localized predominantly at S_4 molecule, in cases when there are lower lying empty orbitals localized at cluster terminating OH groups and Na^+ ions (likely artefact of cluster model). ^fUpon lowering symmetry from D_{2d} to D_2 , $7a_1$ orbital should be relabeled as $9a$, whereas $9e$ split into $9b_2$ (LUMO) and $9b_1$ (LUMO+1). ^gNotable admixture of $O\ 2p$ lattice states to S_4 localized part, see Figure S6. ^hSee Figure S7 below for the explanation of π^* notation.

Figure S5 Differential electron density for the excitation at 371 nm for $C_{2v}(S_4)Na_8Ssod$ model: electron inflow in cyan, outflow in pink.

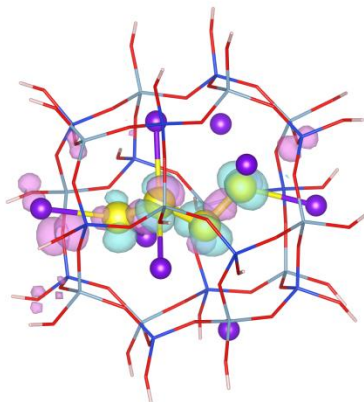


Figure S6 HOMO-1 for $D_{3h}(S_4)Na_8Ssod$ model, see notable mixing of O $2p$ lattice states and S_4 localized part of the orbital.

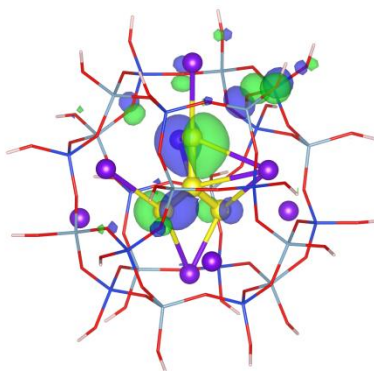


Figure S7 Frontier orbitals in cluster models cut from $trans-(S_4)Na_7Cl$ sod model: HOMO (left) and $LUMO_{S_4}$ (right, i. e. the lowest empty orbital localized primarily on S_4 moiety). Unlike in the ideal C_{2h} symmetry gas phase $trans-S_4$: here HOMO is localized mainly at the longer terminal bond ($S1'-S2'$ atoms), whereas $LUMO_{S_4}$ is localized at shorter bond ($S1-S2$ atoms), both orbitals are π^* type.

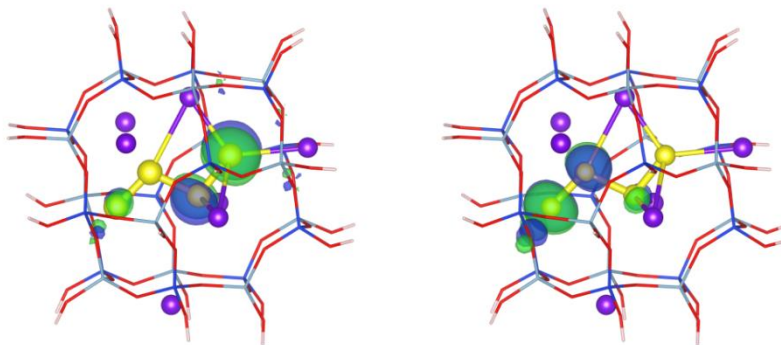


Table S8 Selected TDDFT/LC-BLYP electronic transitions within the range of 350-900 nm for $S_4^{\bullet-}$ chromophores embedded in SOD cages: wavelengths λ and oscillator strengths f_{osc} (in parenthesis), along with the dominant orbital contribution are given. Note that $S_4^{\bullet-}$ isomers and the relevant orbitals are labeled according to the ideal gas phase symmetry of the corresponding $S_4^{\bullet-}$ species (compare with Table 7 in manuscript), the actual symmetry of embedded species is often lower. All transitions within minority spin channel, unless specified otherwise (α subscript).

S_4 isomer	λ (nm), f_{osc}	Excitation character
		($S_4^{\bullet-}$)Na ₈ Cl ₈ od
<i>cis</i> - C_{2v} -1 (C_1) ^a	775 (0.034)	$4b_1$ /SOMO-1/ \rightarrow $4a_2$ /SOMO/ (82%)
	715 (0.006)	$13a_1$ /SOMO-2/ \rightarrow $4a_2$ /SOMO/ (75%)
	359 (0.015)	$12b_2$ /SOMO-1/ \rightarrow $4a_2$ /SOMO/ (11%) $3a_2$ (+O 2p) /SOMO-7, -8/ \rightarrow $4a_2$ /SOMO/ (50%)
<i>cis</i> - C_{2v} -2	890 (0.046)	$4b_1$ /SOMO-1/ \rightarrow $4a_2$ /SOMO/ (91%)
	376 (0.012)	$3a_2$ (+O 2p) /SOMO-3/ \rightarrow $4a_2$ /SOMO/ (50%) $13a_1$ /SOMO-4/ _{S4} \rightarrow $4a_2$ /SOMO/ (17%)
		$\pi^*_{S1',S2'}$ /SOMO-1/ \rightarrow $\pi^*_{S1',S2}$ /SOMO+3,+4/ (67%) ^c $(3p)_{S1',S2'}$ \rightarrow $(3p)_{S1}$ ^d
C_s	730 (0.008)	$20a'$ /SOMO-3/ \rightarrow $12a''$ /SOMO/ (62%) $21a'$ /SOMO-1/ \rightarrow $12a''$ /SOMO/ (30%)
	579 (0.011)	$21a'$ /SOMO-1/ \rightarrow $12a''$ /SOMO/ (55%) $20a'$ /SOMO-3/ \rightarrow $12a''$ /SOMO/ (24%)
	403 (0.055)	$19a'$ /SOMO-5/ \rightarrow $12a''$ /SOMO/ (59%) $21a'$ /SOMO-1/ \rightarrow $12a''$ /SOMO/ (10%)
C_{3v}	714 (0.058)	$10e$ /SOMO-1/ \rightarrow $11a_1$ /SOMO/ (89%)
	494 (0.030)	$9e$ /SOMO-2/ \rightarrow $11a_1$ /SOMO/ (74%)
		($S_4^{\bullet-}$)Na ₇ sod
<i>cis</i> - C_{2v} -1	795 (0.058)	$4b_1$ /SOMO-1/ \rightarrow $4a_2$ /SOMO/ (92%)
	352 (0.022)	$3a_2$ (+O 2p) /SOMO-3/ \rightarrow $4a_2$ /SOMO/ (>45%)
<i>cis</i> - C_{2v} -2 (C_1) ¹	669 (0.034)	$4b_1$ /SOMO-1/ \rightarrow $4a_2$ /SOMO/ _{S4} (91%)
	369 (0.012)	$3a_2$ (+ O 2p) /SOMO-4, -5/ \rightarrow $4a_2$ /SOMO/ (44%) $12b_2$ /SOMO-1/ _{α} \rightarrow $13b_2$ /SOMO+9/ _{α} (21%)
C_{3v} (C_1) ¹	755 (0.037)	$10e(a')$ /SOMO-1/ \rightarrow $11a_1$ /SOMO/ (89%) ^e
	487 (0.023)	$9e(a'')$ (+ O 2p) /SOMO-7, -10/ \rightarrow $11a_1$ /SOMO/ (56%) ^e $10e(a'')$ /SOMO-2/ \rightarrow $11a_1$ /SOMO/ (21%) ⁵
	437 (0.015)	$9e(a')$ (+ O 2p) /SOMO-12,-13,-14/ \rightarrow $11a_1$ /SOMO/ (75%) ^e

^aThe actual symmetry of embedded $S_4^{\bullet-}$ radical in parenthesis. ^bConverged from initial C_{2h} geometry. ^cSee Figure S8, for the explanation of π^* notation. ^dTransition involving multiple pairs of MO, hence difficult for analysis in terms of MO, see excitation difference density in Figure S9 below. ^e a'/a'' in parenthesis denotes the components of e orbitals (within ideal C_{3v} symmetry) which are symmetrical/antisymmetrical with respect to vertical mirror plane.

Figure S8 Orbitals participating in 758 nm excitation in *gauche*- C_2 -(S_4^{\bullet}) Na_8Cl_{10} model: SOMO, localized mainly at the longer terminal bond (S1'-S2'), along with SOMO+3 and SOMO+4, localized at the shorter terminal bond (S1-S2), all orbitals are of π^* type.

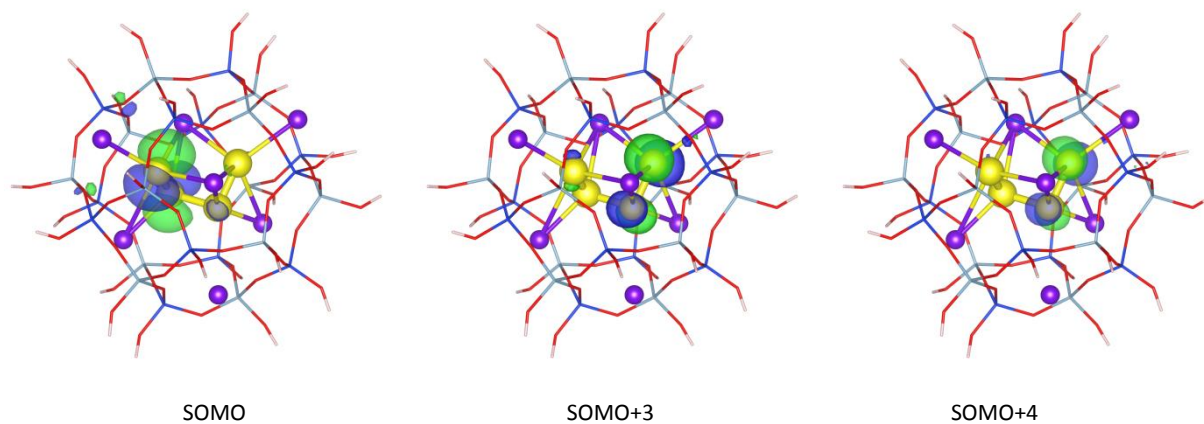


Figure S9 Differential electron density for the excitation at 365 nm in *gauche*- C_2 -(S_4) Na_8Cl_{10} model: electron inflow in cyan, outflow in pink.

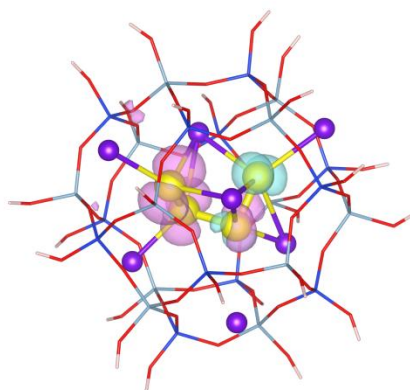
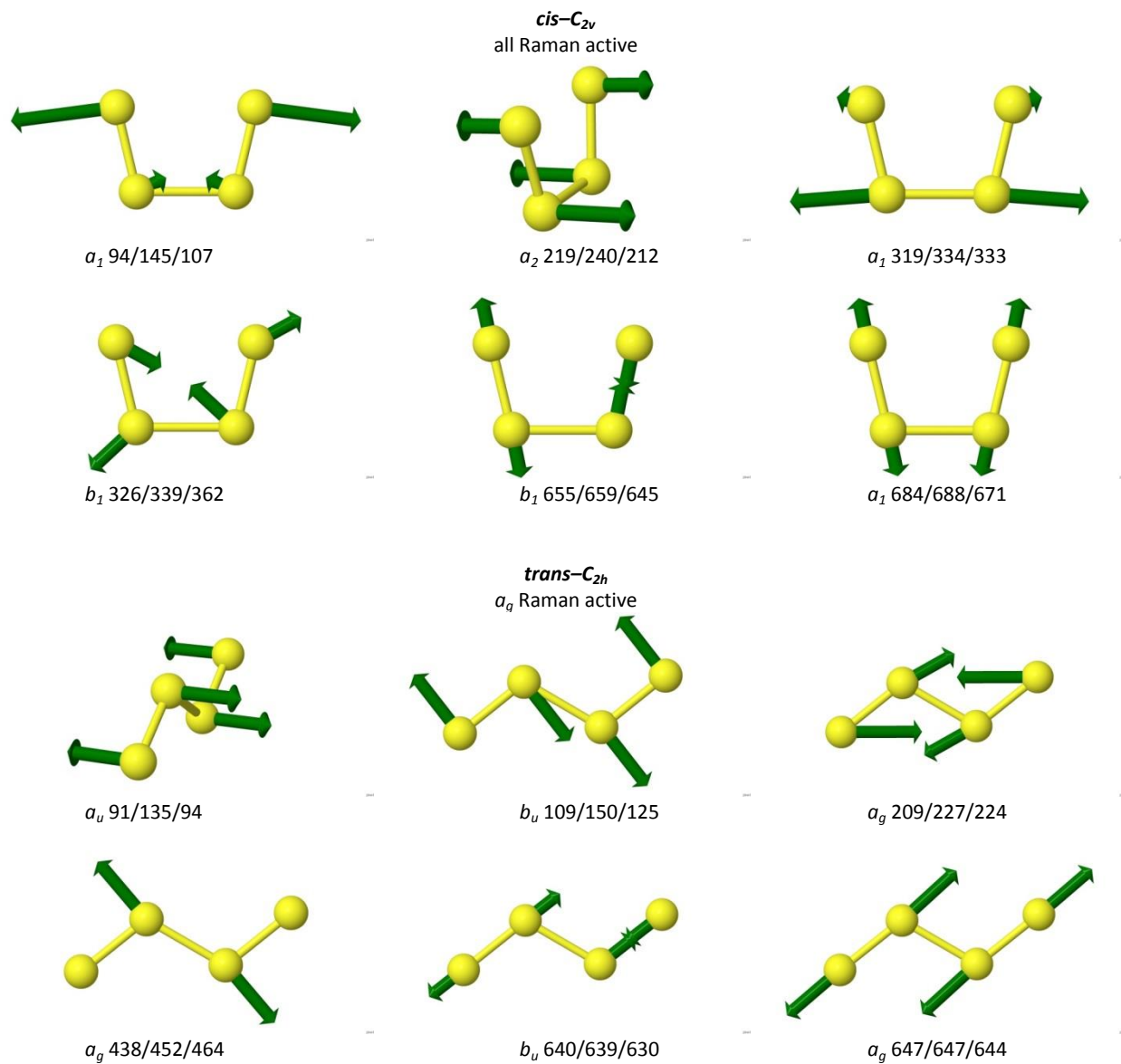
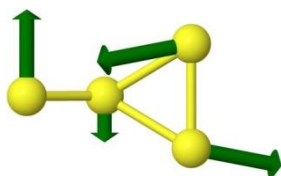


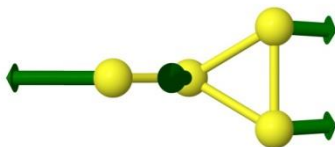
Figure S10 Normal modes for gas phase S_4 molecules at DFT level. The frequencies (in cm^{-1}) are given as (i)/(ii)/(iii), where (i) PBE in def2-TZVP basis set (ORCA), (ii) PBE in PW with $E_{\text{cutoff}}=40$ Ry (Quantum Espresso), and (iii) B3LYP in def2-TZVP basis set (ORCA).



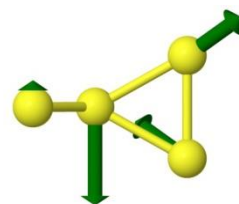
C_s
all Raman active



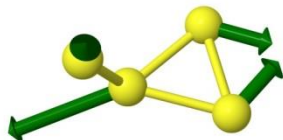
a'' 163/175/166



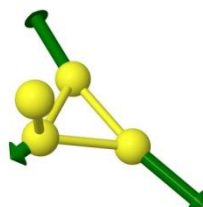
a' 210/220/217



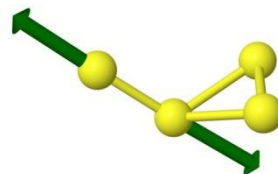
a'' 303/311/306



a' 387/393/386

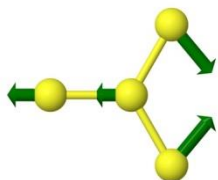


a' 535/544/531

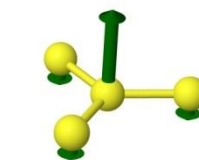
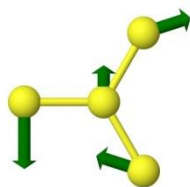


a' 671/670/661

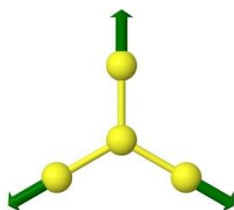
D_{3h}
 a_1' and e' Raman active



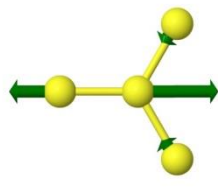
e' 234/237/242



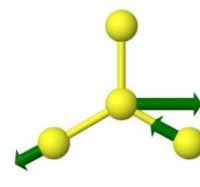
a_2'' 261/258/267

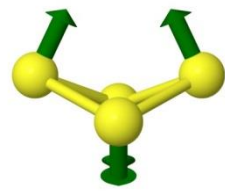


a_1' 466/463/469

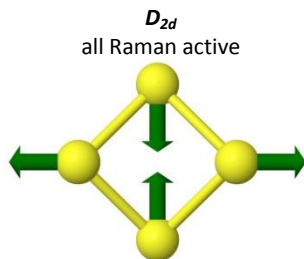


e' 701/697/702

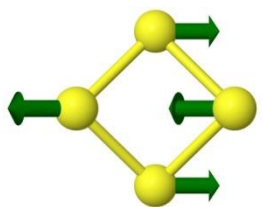




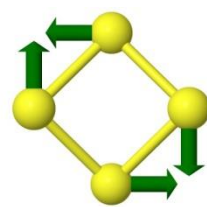
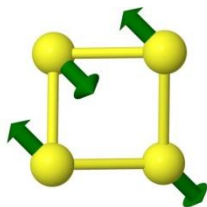
a_1 204/233/199



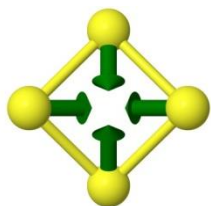
b_2 277/285/299



e 399/424/413

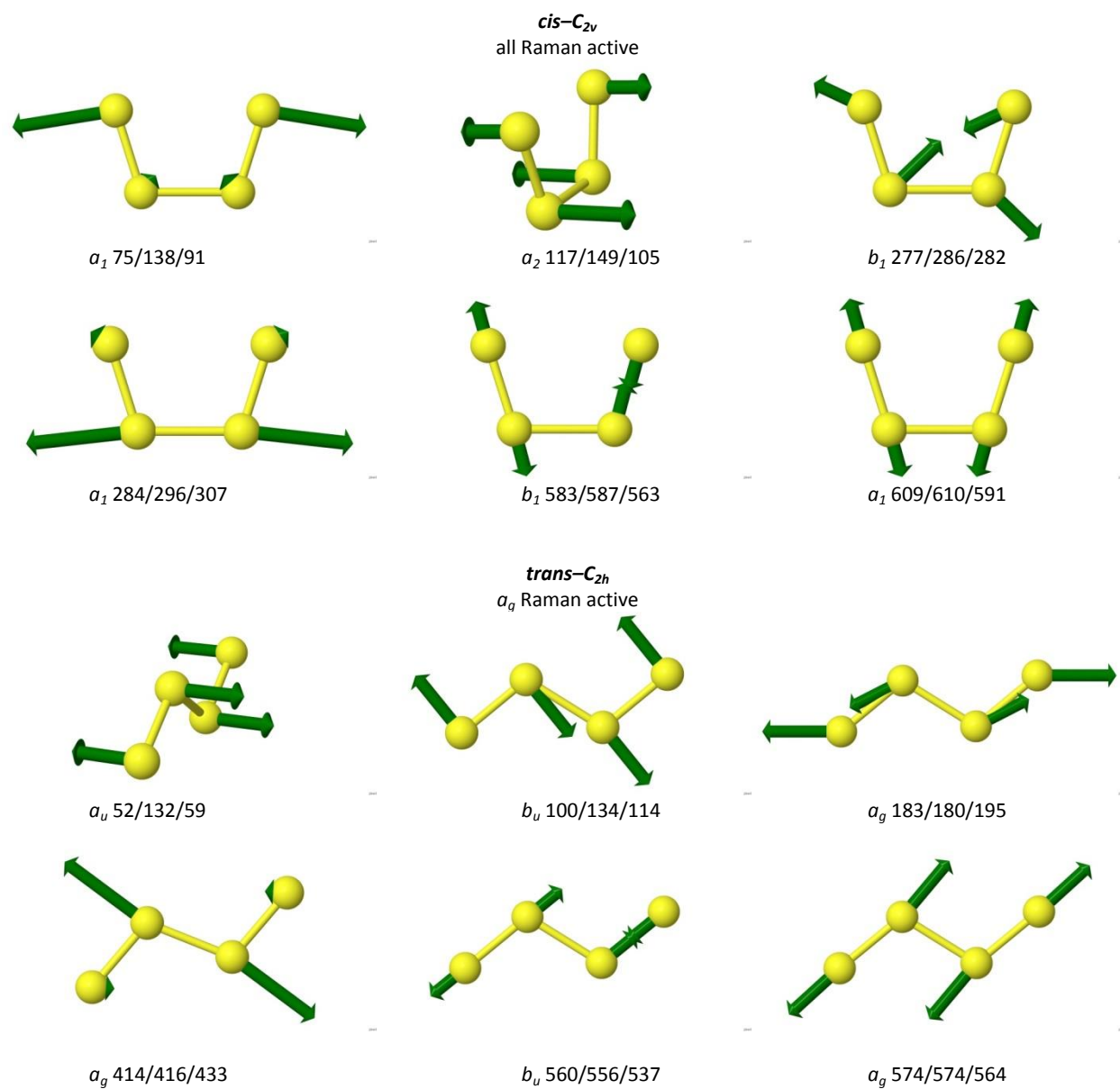


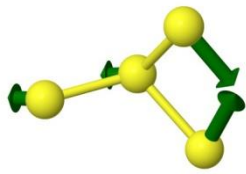
b_1 425/423/440



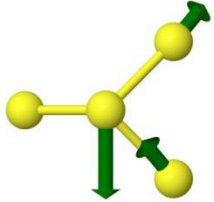
a_1 506/495/504

Figure S11 Normal modes for gas phase $S_4^{\bullet-}$ radicals at DFT level. The frequencies (in cm^{-1}) are given as (i)/(ii)/(iii), where (i) PBE in ma-def2-TZVP basis set (ORCA), (ii) PBE in PW with $E_{\text{cutoff}}=40$ Ry (Quantum Espresso), and (iii) B3LYP in ma-def2-TZVP basis set (ORCA).

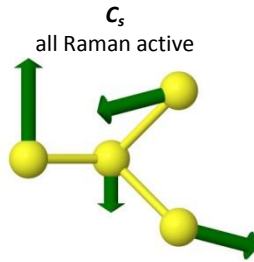




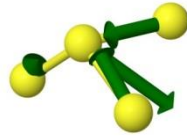
α' 157/185/172



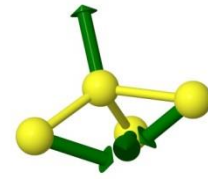
α'' 400/417/406



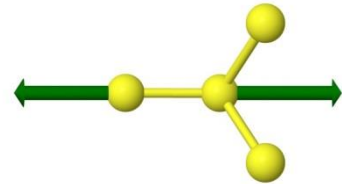
α'' 163/196/173



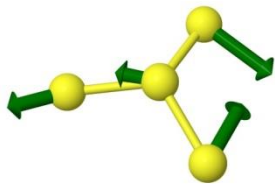
α' 462/483/467



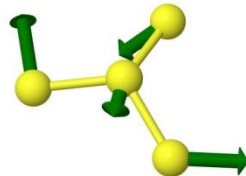
α' 241/241/248



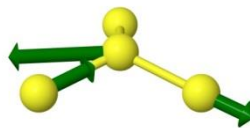
α'' 545/547/534



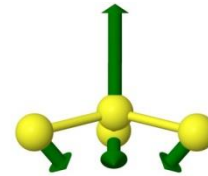
e 200/201/207



α_1 418/417/418



e 554/557/550



α_1 252/251/251

